

M. Vrancken, M.-L. Mayoral, T. Blackman, V.I.V. Bobkov, D. Child, P. Dumortier,  
F. Durodié, M. Evrard, J. Fanthome, R.H. Goulding, M. Graham, S. Huygen,  
P.U. Lamalle, F. Louche, A.M. Messiaen, I. Monakhov, M.P.S. Nightingale,  
J.-M. Noterdaemed, J. Ongena, D. Stork, M. Vervier, A. Walden,  
A. Whitehurst and JET-EFDA Contributors

## Recent ICRF Developments at JET

“This document is intended for publication in the open literature. It is made available on the understanding that it may not be further circulated and extracts or references may not be published prior to publication of the original when applicable, or without the consent of the Publications Officer, EFDA, Culham Science Centre, Abingdon, Oxon, OX14 3DB, UK.”

“Enquiries about Copyright and reproduction should be addressed to the Publications Officer, EFDA, Culham Science Centre, Abingdon, Oxon, OX14 3DB, UK.”

# Recent ICRF Developments at JET

M. Vrancken<sup>1</sup>, M.-L. Mayoral<sup>2</sup>, T. Blackman<sup>2</sup>, V.I.V. Bobkov<sup>4</sup>, D. Child<sup>2</sup>,  
P. Dumortier<sup>1</sup>, F. Durodié<sup>1</sup>, M. Evrard<sup>1</sup>, J. Fanthome<sup>2</sup>, R.H. Goulding<sup>3</sup>, M. Graham<sup>2</sup>,  
S. Huygen<sup>1</sup>, P.U. Lamalle<sup>1</sup>, F. Louche<sup>1</sup>, A.M. Messiaen<sup>1</sup>, I. Monakhov<sup>2</sup>,  
M.P.S. Nightingale<sup>2</sup>, J.-M. Noterdaemed<sup>4,5</sup>, J. Ongena<sup>1</sup>, D. Stork<sup>2</sup>, M. Vervier<sup>1</sup>,  
A. Walden<sup>2</sup>, A. Whitehurst<sup>2</sup> and JET-EFDA Contributors\*

<sup>1</sup>Royal Military Academy, Laboratory for Plasma Physics, Association EURATOM-Belgian State,  
B-1000 Brussels, Belgium

<sup>2</sup>UKAEA/Euratom Fusion Association, Culham Science Centre, Abingdon, OX14 3DB, UK.

<sup>3</sup>Oak Ridge National Laboratory, P.O. Box 2008, MS-6169, Oak Ridge, Tennessee, TN37831-6169, United States

<sup>4</sup>Max-Planck Institute for Plasmaphysics, EURATOM Association, D-85748, Germany.

<sup>5</sup>Ghent University, EESA Department, B-9000 Ghent, Belgium.

\*See annex of J. Pamela et al, "Overview of JET Results",

(Proc.20<sup>th</sup> IAEA Fusion Energy Conference, Vilamoura, Portugal (2004)).

Preprint of Paper to be submitted for publication in Proceedings of the  
SOFT Conference,

(Warsaw, Poland 11th – 15th September 2006)



## **ABSTRACT.**

The Ion Cyclotron Resonance Frequency (ICRF) heating system on JET is currently being upgraded in order to validate new matching concepts in view of coupling ICRF power to ITER plasmas and to further increase the total additional heating power on JET. The present paper reports on first testbed results from the new JET ITER-like antenna, preliminary matching algorithms, as well as on the first use of the newly installed hybrid couplers between two of the existing A2 antennas. Several other on-going improvements, such as improved trip management system, external conjugate-T matching circuit and arc detection systems are also discussed.

## **1. INTRODUCTION**

Coupling high levels of ICRF power into plasmas is a challenging issue both on present-day tokamaks and on ITER. A major difficulty is presented by the very fast (50-200 ms) change in the real and imaginary parts of the ICRF antennas input impedance during Edge Localised Modes (ELMs) [1]. On the JET tokamak, upgrades of the ICRF heating system are currently being implemented, in order to validate different “ELM-tolerant” solutions. Four enhancements are, or will be, implemented as depicted in Fig.1: (1) a new ITER-like antenna with eight internal vacuum capacitor matching elements and four conjugate-T junctions [2], (2) the installation of hybrid couplers between two of the four existing A2 antennas [3] (namely A and B), (3) the improvement of the existing trip management system and (4) the installation of an external (i.e. outside the tokamak vacuum vessel) conjugate-T circuit tuned to low resistive impedance by coaxial line-stretchers (trombones) between the other two A2 antennas (C and D) [4].

Prior to installation of the JET ITER-like antenna on the JET torus planned in 2007, its overall design specifications [5] are to be verified on a separate Radio Frequency (RF) testbed, consisting of a 2m diameter vacuum vessel with extensive diagnostics and of a moveable plexiglas tank filled with water to emulate a variable plasma load [6]. First results from the testbed will be reported in Section 2.

During the 2004-2005 shutdown, hybrid 3dB couplers have been installed between generator B and the antennas A and B. The initial goal was to free one of the generators to power the oncoming JET ITER-like antenna (see Fig.1, note that before their installation generator A was feeding antenna A), but it has become clear that the coupler properties could be used to increase the ICRF power on ELMs as done on ASDEX-Upgrade [7][8]. Experiments have been performed recently and will be presented in Section 3. Other upgrades such as the external conjugate-T (ECT) matching circuit using line stretchers between antennas C and D, improved trip management (ITM) system and arc detection systems will be reviewed in section 4.

## **2. TESTING OF THE JET ITER-LIKE ANTENNA**

The new JET ITER-like antenna, which has arrived on the JET site earlier this year, is composed of four Resonant Double Loops (RDLs) disposed in an array of 2 toroidal by 2 poloidal and each consisting of two poloidally adjacent straps. Each strap will be fed through in-vessel matching capacitors from a

common vacuum transmission line. Although the JET ICRF plant transmission lines and control systems needed to operate the JET ITER-like antenna have been installed and partially commissioned, the antenna itself is first assembled and tested on a testbed prior to commissioning on the JET torus. This preparatory testing consists of three main phases: (1) measurement of the full 8 port antenna strap array scattering matrix at low power in open air with a water load positioned at varying distance to characterize the antenna loading and mutual coupling, and RF probe calibration, (2) high voltage vacuum tests to prepare the antenna for torus-like operating conditions and (3) low power RF matching studies using the moveable water load, in order to validate several matching algorithms to control the capacitor positions from measured RF signals.

## **2.1 STRAP ARRAY MEASUREMENTS**

The initial electrical design of the JET ITER-like antenna [5] was based on engineering estimates of expected strap loading for the most likely L- and H-mode plasma conditions and by neglecting the subtle mutual coupling effects between the individual straps. Although we know that while a conjugate-T solution can still be found with some additional effort, the effects on the expected load resilience of mutual coupling (and geometrical asymmetries) can be more serious [9][10]. It is therefore necessary to confirm experimentally the behaviour of the antenna strap array as predicted by simulations [11]. Plasma-like loading conditions can be emulated by positioning a high dielectric constant medium (where water with dielectric constant  $\mu_r=81$  is convenient) at varying distance of the antenna front strap array as pioneered in [6]. Fig.2 shows part of the testbed experimental setup. The JET ITER-like antenna front box, with Ag coated Al Faraday screen bars and private limiter tiles, is fixed to a metal support frame. The glued plexiglass water tank which has a 2 cm wall thickness, is supported by a second moveable frame on wheels which allows to vary its relative distance to the antenna. The water tank actually consists of 3 separate smaller tanks stacked on top of each other (see Fig.2 right), with a total volume of a 1000 liters, and each contains a salty water solution (5 g salt per liter water gives 0.5 Ohm-1 m-1 conductivity). The salt concentration was determined such that the electromagnetic wave launched from the antenna will be damped and penetrates at worst  $\sim 20$  cm into the water, thus creating a radiation boundary condition instead of a standing wave pattern by reflection on the water tank back wall which would distort the measurement. The full 8 port S-matrix was measured in the 1-200 MHz frequency range for several distances between antenna and water tank using a 4 port network analyser connected to the antenna housing back access ports through appropriate measurement adaptors (see Fig.2 left). The conical 20 to 50 measurement adaptors were characterized separately to subtract their influence (to “de-embed”) from the raw measurement data. Fig.3 (straps numbered as seen looking from the back of the antenna towards the torus centre) shows the reflection coefficients S11 and S22 on ports 1 and 2 as a function of antenna-water tank distance for different frequencies. As expected, it was found that the coupling to the water load increases with increasing frequency and decreasing distance. Note that strap 2 has slightly worse coupling characteristics than strap 1. Contrary to strap 1 (and 4, 5, 8) the middle strap 2 (and 3, 6, 7) has a connection between feeder and strap where

the current actually flows in opposite direction to the current on the strap itself, which causes it to radiate slightly less.

## **2.2 CAPACITOR RF PROBE CALIBRATION**

The voltages at the JET ITER-like antenna vacuum matching capacitors fixed flanges (at the antenna strap end) will be monitored in amplitude and phase by 16 RF “pickup” probes. These RF probe signals will first serve to limit the capacitor voltage amplitude for antenna safety. They will also be used as additional inputs, together with the forward and reflected power on the transmission lines, to control the capacitor positions (see Further Section 2.4) and also in arc detection and protection circuits (see further Section 4). A full RF calibration including the effects of a measurement adaptor, attached cables and junction boxes was performed with a network analyser as represented in Fig.4. The amplitude of the resulting extracted calibration factor  $CF = V_3/V_2$  (with  $V_3$  and  $V_2$  the voltages in the reference planes 2 and 3 defined in Fig.4) as a function of frequency is depicted in Fig.5. and shows the compensation it gives for the increased capacitive coupling from capacitor flange to the probe with increasing frequency. For the maximum allowed capacitor voltage of 45 kV, the corresponding cable voltage will be ~40 V in the 30-55 MHz frequency range.

The slight oscillation on the full RF extraction (full line) compared to an extrapolation from low frequency (dashed line) is due to losses on a ~4 m thermocoax high temperature resistant vacuum cable (from probe to vacuum exit flange at the back of the VTL) and a ~2 m RG223 RF jumper cable (from exit flange to RF junction box attached to the antenna Ex Vessel Support Structure (EVSS)) which creates a slight impedance mismatch, but this effect is taken into account by the full RF calibration procedure.

## **2.3 HIGH POWER TEST PREPARATION**

The JET ITER-like antenna is currently being assembled and prepared for high power tests in vacuum. To do so, a separate 2 m diameter vacuum vessel will be used, with the 2 MW RF power provided by the JET ICRF plant generator A1. The testbed is equipped with several auxiliary features, such as vessel baking capability, vacuum system, water cooling plant, and a hydraulic system to operate the capacitor hydraulically driven actuators. The signals from vacuum gauges, thermocouples, flow meters, pressure sensors, infra-red and visible camera’s, will be monitored in a separate purpose built testbed control room. The signals from the transmission line RF couplers and antenna RF probes will be processed by a matching algorithm that sends control signals to the hydraulic plant to optimise the antenna matching.

## **2.4 RF MATCHING STUDIES**

At present two matching algorithms are proposed to control the position of the JET ITER-like antenna capacitors. The first one only uses the measured admittance along the 4 feeding transmission lines as inputs and attempts to control the admittance at the 4 conjugate T-points to a set of pre-defined values

(which can be complex). The main advantage is that the chosen T-point matching admittances immediately define the settings of the 2nd stage matching circuits [2] at the operating frequency (i.e. these do not change during the ICRF pulse). The main disadvantage is that mutual coupling within the array of 8 straps can cause multiple solutions to exist for a given problem. This can cause the matching algorithm to converge to a mathematical solution with less favourable physical characteristics. Another disadvantage is that the distribution of voltages over the various straps of the array depends on the coupling with the plasma and is largely beyond control, and this may reduce the power that can be delivered to the plasma. The second algorithm uses the RP probe measurements of the capacitor fixed flange voltages and attempts to control the ratio of the voltages at the antenna strap feeders directly. It can be shown that the matching solution is no longer multi-valued and another advantage is that the voltage distribution across the array is controlled directly. However, the disadvantage is now that the admittance at the conjugate-T point is not known beforehand and this requires adjustment of the 2nd stage matching circuit settings during the ICRF pulse. Techniques to determine the operating point that a priori gives the optimal ELM resilience are still under development, by combining theoretical assessment [10] and experimentation on the testbed.

### **3. PERFORMANCE OF 3DB SPLITTERS ON JET-A2 ANTENNAS**

The hybrid (3 dB) couplers installed to split the power from generator B between antennas A and B, are fourport networks that have the property to isolate the generators from reflected power coming back from the antenna. Indeed if two of the ports are terminated in arbitrary but identical impedances, and the third port is terminated in a matched load, then the fourth port is matched. The relative phase between the incident voltage in the two output ports is  $90^\circ$ . On JET, the couplers have been installed in such a way that the two output ports are connected to similar straps of antenna arrays A and B and the fourth ports are connected to the generator amplifiers (see Fig.6). It was then expected that during ELMs, if the change in loading results in identical change in impedance for the two output ports of the couplers, referred as the Splitter Transmission Lines (STLs), the reflected power will go to the load instead of going to the Output Transmission Line (OTL), avoiding tripping of the generator for protection. The need for the two arbitrary impedances (and their changes) to be identical is quite important and requires low mutual inductance (e.g. straps sufficiently far from each other or separated by a septum). The straps, however, cannot be too far from JET, ELMs do not appear simultaneously toroidally around the machine [12]. In parallel to the coupler installation the data acquisition has been upgraded to obtain the forward and reflected voltage amplitudes on the OTLs and STLs with a resolution up to  $4 \mu\text{s}$ . Typical results are shown on Fig.7 and Fig.8 during type I ELMs. On Fig.7, one can clearly see the change in coupling resistance during each ELM. The A1 and B1 STLs were initially matched, nevertheless neither the stub position or frequency feedback loop forming the JET matching system [13] could react fast enough as can be seen on the increase in A1 and B1 STL reflected powers (see Figs.7b and 7c). Nevertheless, due to the presence of the 3dB couplers, the STLs reflected powers were successfully directed to the 3dB coupler load (see Fig.7d) instead of the OTL. As almost no

reflected powers were seen on the OTL, the generators were not tripped, as they would have been prior to the installation of the 3 dB couplers. The total coupled power from the four A2 antennas is represented on Fig.8. During this pulse, 65 trips were counted for antenna C, 130 for antenna D and 2 for antennas A and B, clearly showing an improvement in the averaged coupled power with the presence of the 3dB couplers. Nevertheless, during these first tests, a few problems were encountered preventing to go to higher power. First of all, as illustrated on Fig.8 by the peaks in coupled power from antennas A and B, a problem with the RF local manager controlling the feedback loop for the coupled power was observed. More importantly, in order for the STL reflected power to reach the couplers, it was necessary to change the level of protection against arcs which is based on measurements of the voltage standing wave ratio (VSWR) both on the STLs and OTLs. It was found that the VSWR protection levels used were not satisfactory and were putting the ICRF plant at risk. These levels have been recently adapted and further tests at higher ICRF power should be done possibly in the near future.

#### **4. ONGOING ENHANCEMENTS**

Finally, successful results from the ECT prototype [4] installed in 2003 between one pair of adjacent straps of the antenna C have led to a new project. The conversion of this prototype into a transmission line layout suitable to be installed between the complete antennas C and D has been completed. For the actual installation, about 80% JET surplus transmission line components will be re-used while orders for an additional 20% new components and upgrade electronics have been placed.

The work for the installation is currently being planned and intended to be completed in the forthcoming shutdown.

In parallel, the electronics controlling the trip time of the generator during high reflected power due to arcs or ELMs is being upgraded in order to reapply power more quickly in case of an ELM-triggered trip. The improved trip management system [14] attempts to distinguish between arcs and ELMs looking at the  $D_{\pm}$  line emission intensity signal, and applies a much shorter trip and recovery period in case of an ELM. A first version of the software has been tested successfully on half of antenna A and should be implemented on antenna D in the near future.

However, all present ICRF systems remain prone to electrical arcing. For example the occurrence of arcs in the JET A2 VTLs or the JET ITER-like antenna conjugate T-point remains undetected by any VSWR based system due to the low voltage at these locations. Several new arc detection systems independent of the VSWR protection are under consideration:

- S-Matrix or signal consistency Arc Detection (SMAD), for which additional measurement points (such as the RF probes on the JET ITER-like antenna) close to the antenna straps are required,
- Sub-Harmonic Arc Detection (SHAD), which looks for a characteristic sub-operating frequency band noise signature (which even occurs slightly ahead) of the arc [15],
- Optical arc detection, which detects visual and UV light occurring inside the antenna housing and VTL through a system of mirrors and optical fibres.

All of these systems are scheduled to be tested on the JET ITER-like antenna testbed as well.

## CONCLUSIONS

Dealing with the strong and fast ICRF antenna loading variations during ELMy plasmas has been an issue for years. Several ELM-tolerance techniques are being or will be tested at JET in the next few months. In particular, the new JET ITER-like antenna is being installed on its testbed and first strap array measurements have been performed. High power vacuum testing and low power testing with a water load of the RF matching algorithms will follow shortly. In parallel, the ELM tolerance of the newly installed 3dB couplers has been successfully tested on antenna A and B at low power. Further experiments are planned at higher power.

## ACKNOWLEDGEMENTS

This work was carried out within the framework of the European Fusion Development Agreement. The views and opinions expressed herein do not necessarily reflect those of the European Commission. The work carried out by UKAEA personnel was jointly funded by the UK Engineering and Physical Sciences Research Council and EURATOM.

## REFERENCES

- [1]. J.-M. Noterdaeme *et al.*, “Matching to ELMy plasmas in the ICRF domain”, *Fusion Eng. Des.* **74** (2005)191-198.
- [2]. F. Durodié *et al.*, “Main Design Features and challenges of the ITERlike ICRF antenna for JET”, *Fusion Eng. Des.* **47** (2005) 223-228.
- [3]. A. Kaye *et al.*, “Present and future JET ICRF antennae”, *Fusion Eng. Des.* **24** (1994) 1-21.
- [4]. I. Monakhov *et al.*, “Tests of load-tolerant external conjugate-T matching system for A2 ICRF antenna at JET”, *Fusion Eng. Des.* **74** (2005) 467-471.
- [5]. F. Durodié *et al.*, “JET-EP ITER-like ICRF antenna”, in: 14th Topical Conference on Radio Frequency Power in Plasmas, Oxnard, California, 7-9 May 2001, p. 122-125, AIP Conference Proceedings, vol. 595, Melville, New York, 2001.
- [6]. A. Messiaen *et al.*, “Realisation of a test facility for the ITER ICRH antenna plug-in by means of a mock-up with salted water load”, *Fusion Eng. Des.* **74** (2005) 367-375.
- [7]. J.-M. Noterdaeme *et al.*, “ICRF heating results in ASDEX Upgrade and W7-AS”, in: 16th IAEA Conference on Fusion Energy, vol. **3**, Montreal, 1996, IAEA 335-342.
- [8]. F. Hofmeister *et al.*, “Matching considerations in an ICRH-system with hybrid couplers”, in: 20th Symposium on Fusion Technology, Marseille, Assoc. Euratom-CEA, 1998, pp. 437-440.
- [9]. G. Bosia, S. Bremond, L. Colas, “Effects of coupling and asymmetries on load resilience of IC ITER-like structures”, in: 16th Topical Conference on Radio Frequency Power in Plasmas, Park City, Utah, 11-13 April 2005, p.178-181, AIP conference proceedings, vol. 787, Melville, New York, 2005

- [10]. P.U. Lamalle *et al.*, “Study of Mutual Coupling Effects in the antenna array of the ICRH plug-in for ITER”, *Fusion Eng. Des.* **74** (2005) 359- 365.
- [11]. P.U. Lamalle *et al.*, ”Three-Dimensional Electromagnetic modelling the JET ITER-like ICRF antenna”, in: 15th Topical Conference on Radio Frequency Power in Plasmas, Moran, Wyoming, 19-21 May 2003, p.118-121, AIP conference proceedings, vol. 694, Melville, New York, 2005
- [12]. V. Bobkov *et al.*, “Studies of ELM toroidal asymmetry using ICRF antennas at JET and ASDEX Upgrade”, in: 31st EPS Conference on Plasma Physics, London, EPS, 2004.
- [13]. T.J. Wade *et al.*, “Development of the JET ICRH plant”, *Fusion Eng. Des.* **24** (1994) 23-46, 1994.
- [14]. I. Monakhov *et al.*, “New Techniques for the improvement of the ICRH system ELM tolerance on JET”, in: 15th Topical Conference on Radio Frequency Power in Plasmas, Moran, Wyoming, 19-21May 2003, p.149-153, AIP conference proceedings, vol. 694, Melville, New York, 2005.
- [15]. F. Braun, “An ARC detection system for ICR-heating”, in: 19th symposium on Fusion Technology, Lisbon, 16-20 September 1996. p. 601-603.

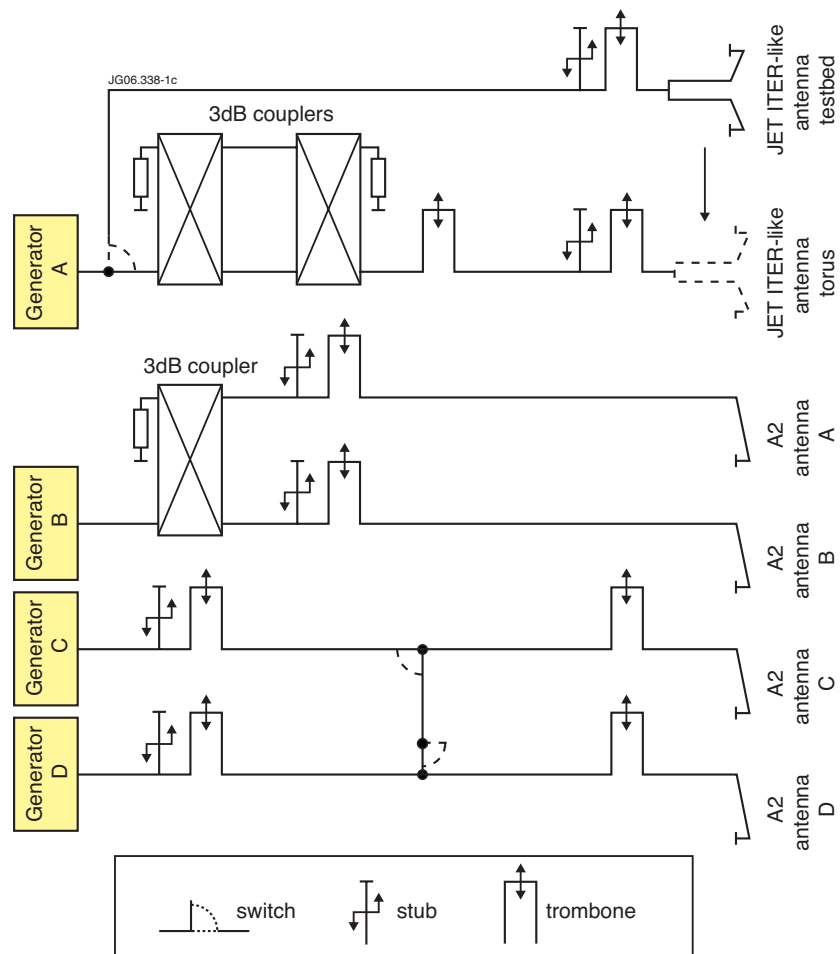


Figure 1: Simplified overview of the present reconfigured JET ICRF system. Each A2 antenna A,B,C,D consists of 4 straps linked by 4 transmission lines to the 4 amplifiers of a generator. The JET ITER-like antenna has a total of 8 straps in a single array and is fed by a single feeding line on the testbed, but 4 when installed on the JET torus.



Figure 2: Left: back view of the JET ITER-like antenna housing with 8 attached measurement adaptors. Right: front view of the JET ITER-like antenna and moveable plexiglass water tank filled with salty water solution.

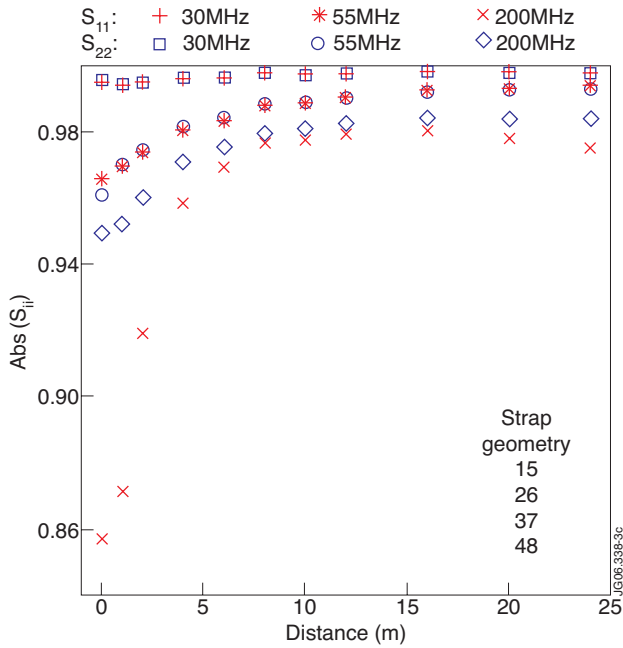


Figure 3: Measured and de-embedded (effect of measurement adaptors subtracted) amplitude of the reflection coefficient for straps 1 and 2,  $S_{11}$ , and  $S_{22}$  respectively, as a function of antenna-water tank distance at three different frequencies 30, 55 and 200MHz.

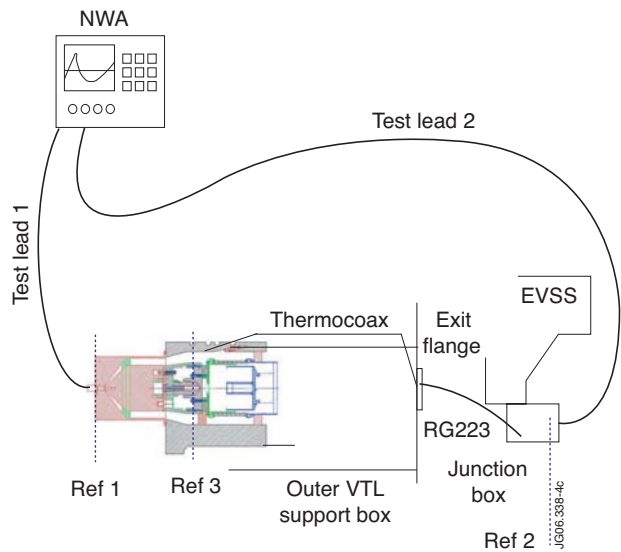


Figure 4: Measurement setup for the capacitor RF probe calibration with insertion of a measurement adaptor, dummy capacitor and short circuit support ring into the capacitor housing. With this setup, all effects of a thermocoax high temperature resistant vacuum cable built into the outer VTL, RG223 RF jumper cable and transitions in the vacuum exit flange and RF junction box attached to the antenna Ex-Vessel Support Structure (EVSS) can be taken into account fully.

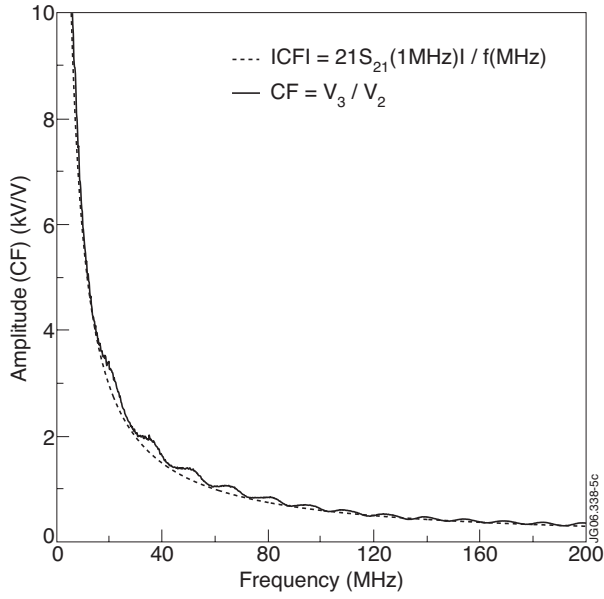


Figure 5: Amplitude of the extracted calibration factor CF (full line) and an extrapolation from a low frequency measurement (dashed line) as a function of frequency. CF will be used to obtain the true voltage at the fixed capacitor electrode in amplitude and phase from the measured voltage at the RF probe cable end.

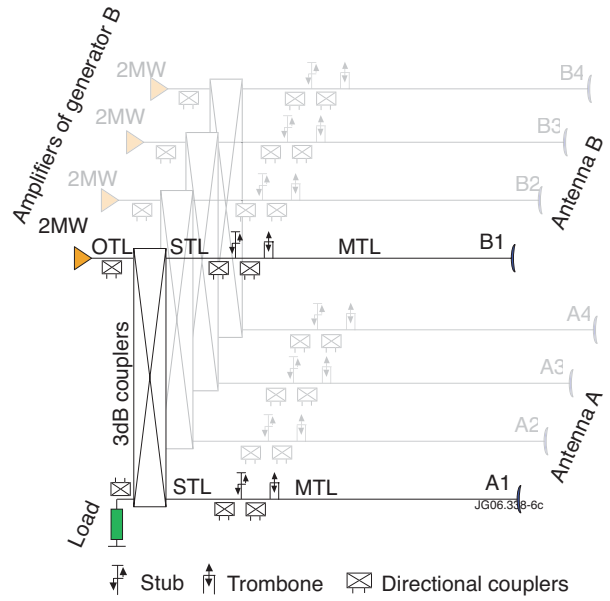


Figure 6: Antenna A and B layout after the hybrid couplers installation. The different parts in the transmission line are referred as the Output Transmission Line (OTL), the Splitter Transmission Line (STL) and the Main Transmission Line (MTL).

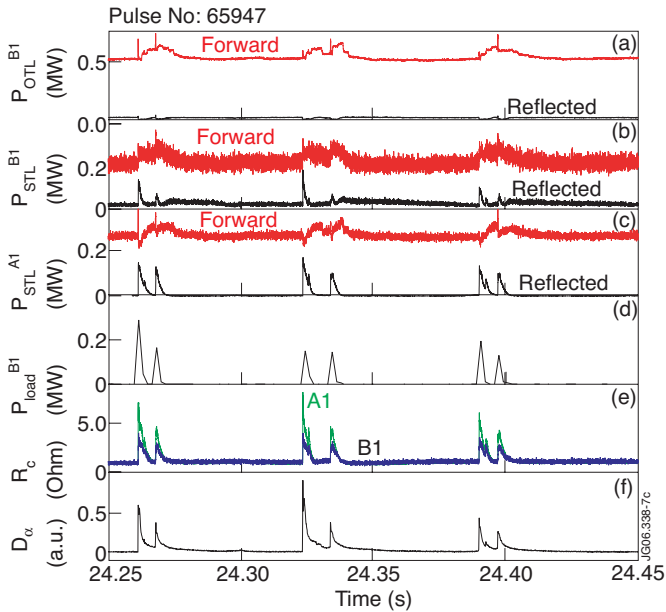


Figure 7: (a) B1 OTL forward and reflected power, (b) B1 STL forward and reflected power (c) A1 STL forward and reflected power, (d) power going to load, (e) A1 and B1 coupling resistance and (f)  $D_{\alpha}$  line emission intensity. Note that the time resolution of the forward and reflected power was in this pulse 20ms and the time resolution for the power going to the load was only 3ms.

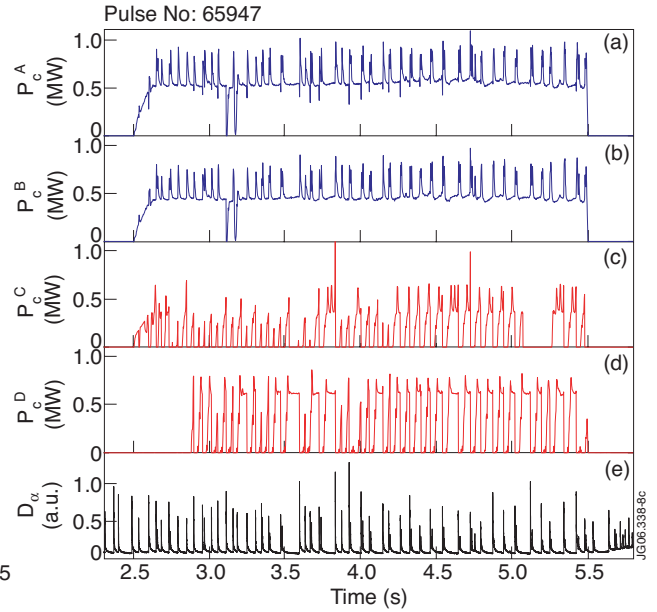


Figure 8: Coupled powers from antenna (a) A, (b) B, (c) C, (d) D and (e)  $D_{\alpha}$  line emission intensity.